

Far-infrared properties of *ab*-plane oriented $\text{YBa}_2\text{Cu}_3\text{O}_{7-\delta}$

D. A. Bonn, A. H. O'Reilly, J. E. Greedan, C. V. Stager, and T. Timusk
Institute for Materials Research, McMaster University, Hamilton, Ontario, Canada L8S 4M1

K. Kamarás and D. B. Tanner
Department of Physics, University of Florida, Gainesville, Florida 32611
 (Received 11 September 1987)

Polycrystalline samples of $\text{YBa}_2\text{Cu}_3\text{O}_{7-\delta}$ with a variety of surface treatments show differences in absolute reflectance and width of phonon lines. Samples that are not polished and are measured immediately after annealing have largely grains with the *c* axis normal to the surface. Such oriented samples show a gaplike depression of conductivity in the far infrared that sets in below the superconducting transition temperature but no true gap. Phonon lines at 195 cm^{-1} and at 155 cm^{-1} narrow in the superconducting state, in analogy with the effect of the electron-phonon interaction in Bardeen-Cooper-Schrieffer superconductors. In the normal state the background conductivity is Drude-like with a plasma frequency of 0.75 eV and a relaxation rate of 200 cm^{-1} . The extrapolated far-infrared conductivity agrees with the measured dc conductivity.

INTRODUCTION

In the following paper, we report on recent improvements in the measurement of the far-infrared optical properties of polycrystalline $\text{YBa}_2\text{Cu}_3\text{O}_{7-\delta}$. In the context of ordinary Bardeen-Cooper-Schrieffer (BCS) superconductivity this spectral region includes the energy gap as well as the excitations responsible for superconductive pairing. Theories of nonconventional superconductivity are characterized by zeroes in the gap function (*d*-state pairing) or by no gap at all (Bose condensation of preexisting pairs). Initial attempts at measuring the energy gap of superconducting $\text{YBa}_2\text{Cu}_3\text{O}_{7-\delta}$ in the far infrared revealed a complex reflectance spectrum with very strong optically active phonons.¹⁻⁵ A study of oriented samples is useful in deciphering the unusual behavior of this material in the far infrared and demonstrates some of the difficulties in interpreting reflectance measurements.

EXPERIMENTS

Three different samples were used in the study. All had the bulk composition of $\text{YBa}_2\text{Cu}_3\text{O}_{7-\delta}$ and were prepared in the usual way.¹ The surface treatments, however, were different. Sample A, the polished sample, was used in the results reported in Ref. 1 and was polished with μm -grit alumina in benzene before making the reflectance measurements. Samples B and C were not polished, but, sample B was exposed to air for several days before the measurements were made, whereas sample C was annealed at 900°C in oxygen, then cooled in an oxygen atmosphere and measured immediately.

Figure 1 shows the x-ray powder diffraction pattern of the surface of sample C compared with the corresponding pattern of a truly random powder sample. Note the significant enhancement of the $(00l)$ reflections relative to the reflections of the type $(hk0)$, $(h0l)$, and $(0kl)$. Clearly this indicates that the sample surface is comprised predominantly of crystallites which are oriented with the *c*

axis normal to the surface. As the x-ray penetration is of the order of $100\ \mu\text{m}$ while that of the far-infrared photons is of the order of 1 to $10\ \mu\text{m}$ the reflectivity experiment obviously probes the highly oriented surface region. From an examination of the relative intensities the fraction of crystallites with *c*-axis orientation normal to the surface is estimated at about 80%.

The high degree of surface orientation is evident in the scanning electron microscope picture shown in Fig. 2. The surface grains are platelike and appear to have grown together in many places to form a continuous surface with few gaps and pits. The average grain size is about $10\ \mu\text{m}$. An elemental analysis shows that the large grains have the 1:2:3 composition. In some sections of the sample there are smaller micron-size particles that contain platinum as well as CuO needles. These minor constituents of the surface occupy an area that is less than 1%.

Great care has been taken to determine the absolute value of the reflectance of each sample. Initially, the sample reflectance is measured against a stainless-steel reference mirror. Then a lead film is deposited on the sample *in situ* at low temperature and the reflectance of the lead-coated sample is measured against the reference mirror. Dividing the initial sample reflectance by the lead-coated sample reflectance corrects for any light that is incoherently scattered from the rough sample surface. This correction is particularly important for freshly annealed surfaces which tend to be rougher than polished surfaces. The ratio gives the reflectance of the sample divided by that of lead, so that a final correction is made for the reflectance of lead. Since lead is a superconductor its absolute, reflectance at 20 cm^{-1} can be determined. We checked our calibrations by studying the temperature-dependent reflectance of stainless steel which, we found, followed Drude theory quite accurately. The dc conductivity agreed with the conductivity determined from the optical measurements. Our procedure gives an absolute value with an error of about $\pm 0.5\%$.

Figure 3 shows the far-infrared reflectance of the three

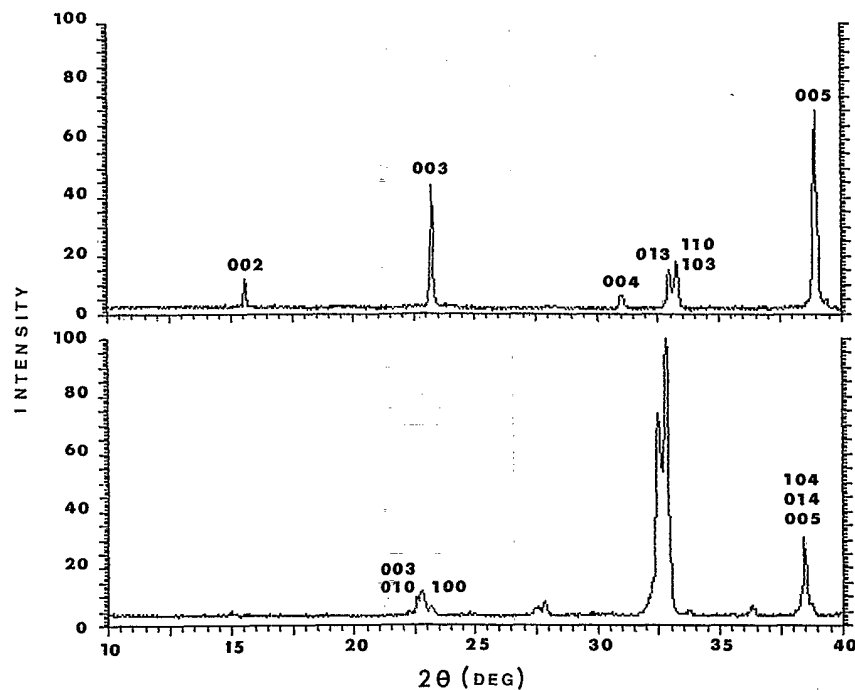


FIG. 1. Part of the diffraction pattern sample C (upper curve) compared with a nearly random powdered sample (lower curve) of $\text{YBa}_2\text{Cu}_3\text{O}_{7-\delta}$. The $(00l)$ reflections are stronger in the bulk sample indicating a substantial orientation of the surface grains. The upper curve is displaced slightly to higher angles due to the placement of the pellet surface relative to the center of the goniometer.

samples of $\text{YBa}_2\text{Cu}_3\text{O}_{7-\delta}$ in the normal and superconducting states. Except for the variation in the overall absolute value and details of the shape of spectral features, the spectra in the normal state are similar for all three samples and are in qualitative agreement with measurements made by other groups.²⁻⁵ All normal-state spectra of this material exhibit an overall Drude-like decreasing reflectance due to free carriers and a set of sharper features due to optically active phonons. Of the three samples the oriented sample C stands out. The reflectance

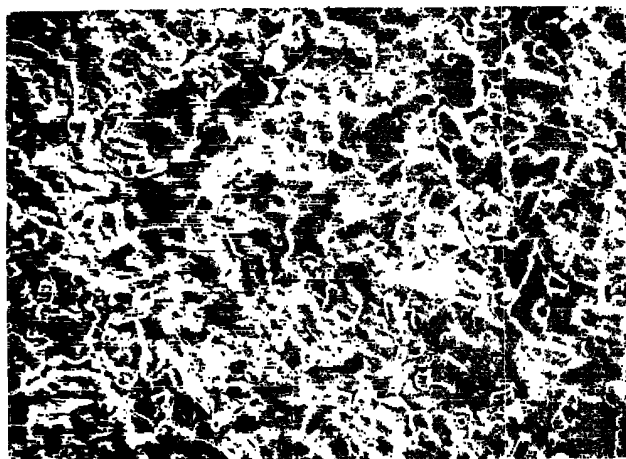


FIG. 2. Scanning electron microscope image of the surface of the highly oriented sample. The flat grains are oriented with their *ab* planes parallel to the surface.

is much higher and the phonon features are sharper in this sample than samples which have been polished or exposed to air for an extended period of time. The reflectance of sample C is high enough to be in reasonable agreement with the measured dc resistivity. Below 80 cm^{-1} the normal-state reflectance can be fit with the Hagen-Rubens expression with a resistivity of $0.4\text{ m}\Omega\text{ cm}$ while the measured resistivity of the sample at 100 K was about $0.3\text{ m}\Omega\text{ cm}$.

In the superconducting state there is a qualitative difference between sample A, the mechanically polished one and samples B and C. For instance, in sample A there is a sharp drop in the reflectance above 70 cm^{-1} whereas the drop in reflectance does not occur until higher frequency in B and C. All three samples are bulk superconductors above 90 K and the major changes in reflectance coincide with the superconducting transition. For instance, measurements of the average reflectance at frequencies below 200 cm^{-1} show that the reflectance follows a mean-field-type behavior. That is, the reflectance abruptly starts to change at about 90 K and exhibits its most rapid changes between 90 and 60 K . Thus, although there is a great deal of sample dependence, the temperature-dependent changes in reflectance of all three samples are associated with the onset of superconductivity.

The sample-to-sample variation of the frequency at which the reflectance sharply drops highlights the danger of trying to associate features in the reflectance spectrum with the superconductor's energy gap. The drop at 70 cm^{-1} in sample A is due to a zero crossing of the real part of the dielectric constant, ϵ_1 , similar to that found in

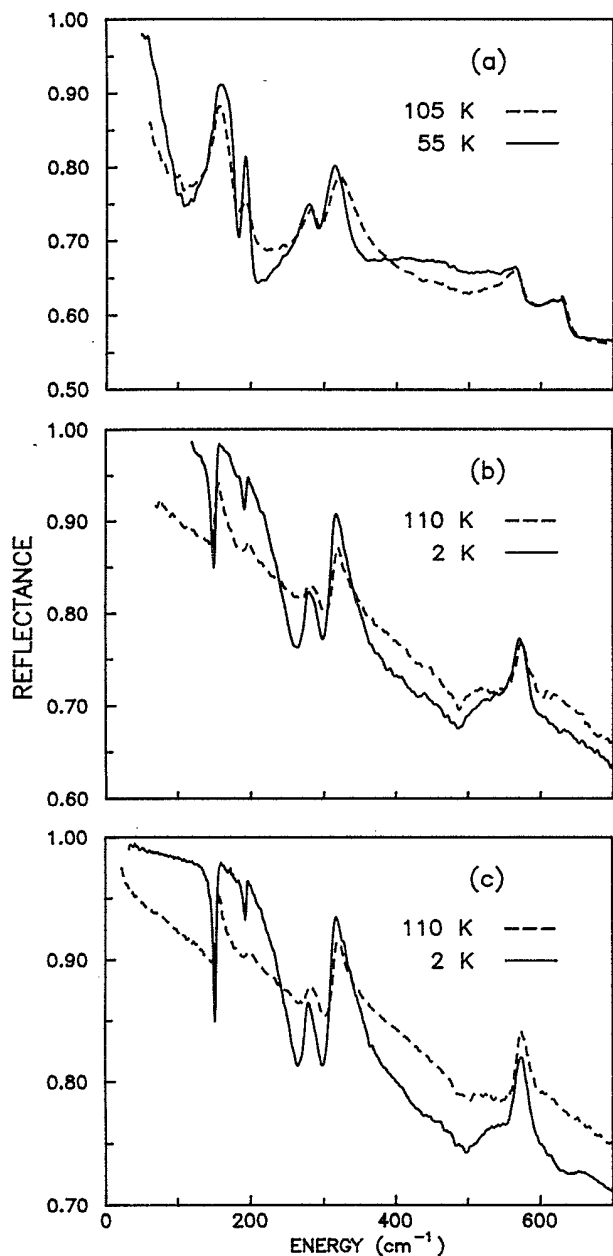


FIG. 3. Reflectance of $\text{YBa}_2\text{Cu}_3\text{O}_{7-\delta}$ in the normal state (solid curves) and in the superconducting state (dashed curves). (a) Sample A: polished surface; (b) sample B: unpolished surface after several days of exposure to air; (c) sample C: unpolished surface immediately after annealing in oxygen.

$\text{La}_{2-x}\text{Sr}_x\text{CuO}_4$.⁶ In samples B and C, ϵ_1 takes on larger negative values and does not exhibit a zero crossing at such low frequencies; hence, the sharp feature at 80 cm^{-1} is not present in these samples. Reflectance measurements have been reported in the superconducting state by other workers and they are in qualitative agreement with the spectra of samples B and C.²⁻⁵ It is evident from Kramers-Kronig analysis or from fits of reflectance to oscillator models that one cannot associate the downturns in reflectance at 150 , 200 , and 320 cm^{-1} with possible ener-

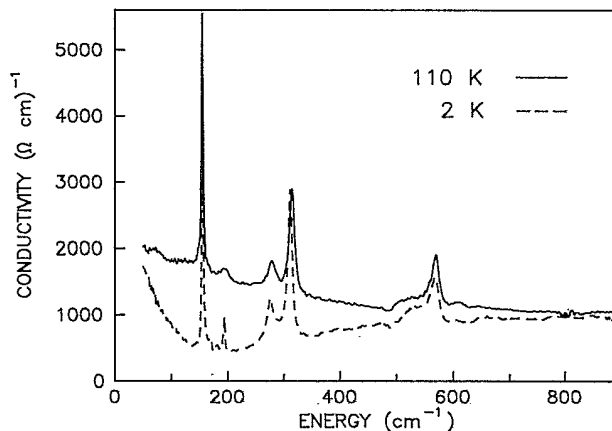


FIG. 4. Real part of the conductivity of $\text{YBa}_2\text{Cu}_3\text{O}_{7-\delta}$ in the normal state (solid curve) and in the superconducting state (dashed curve) from Kramers-Kronig analysis of the reflectance of sample C (unpolished and freshly annealed in oxygen). We consider the suppression of low far-infrared conductivity at the superconducting transition and the narrowing of low-lying phonon lines evidence for the existence of an energy gap.

gy gaps.

It is also misleading to use the temperature dependence of the reflectance at the superconducting transition to find the energy gap: The presence of phonon features that change in width and energy upon cooling into the superconducting state confuse any attempt to determine the energy gap directly from the reflectance. The two reasonable methods of extracting information from these spectra are fitting the reflectance to a model of the dielectric properties of the material or Kramers-Kronig analysis. The latter technique, which is used to analyze the data presented here, has the disadvantage that it is strictly correct for wavelengths long compared to particle size, typically $10\text{ }\mu\text{m}$. In this long-wavelength region an effective dielectric constant of the medium can be defined⁷ to account for the inhomogeneous nature of these polycrystalline samples. The Kramers-Kronig method has the substantial advantage that one need not assume a particular model with which to fit the data.

Figure 4 shows the real part of the conductivity of sample C as obtained by Kramers-Kronig analysis of the reflectance. In the normal state the conductivity is composed of a set of sharp absorption features superimposed on a smooth background conductivity which decreases with increasing frequency. At the low-frequency end the conductivity is about $2100\text{ }(\Omega\text{ cm})^{-1}$, which is in reasonable agreement with the measured dc conductivity of $3300\text{ }(\Omega\text{ cm})^{-1}$. The leveling off of the conductivity above 600 cm^{-1} is caused by the low-frequency tail of the large absorption feature seen at 3000 cm^{-1} by Kamarás *et al.*⁸ A good fit of normal-state background conductivity is obtained if one simply uses the Drude expression for conductivity due to free electrons, $4\pi\sigma(\omega) = \omega_p^2\tau/(1 + \omega^2\tau^2)$, plus a correction for the tail of the feature at 3000 cm^{-1} . Although the free-electron parameters obtained in this way are sensitive to the shape assumed for the high-frequency structure, one can give a reasonable range for them by trying a variety of fits with tails of different

shapes. The value of the scattering rate obtained by this analysis is in the range of 200 to 400 cm^{-1} , which can be seen as the characteristic frequency over which the normal-state conductivity is decreasing. The plasma frequency is in the range of 4000 to 8000 cm^{-1} . For the subsequent discussion we will adopt a plasma frequency of 5000 cm^{-1} (0.75 eV) and a scattering rate $1/\tau = 300 \text{ cm}^{-1}$.

Below the superconducting transition temperature, the overall conductivity becomes depressed in the far infrared and the sharp absorption features exhibit a variety of changes. The rapid rise in the conductivity below 130 cm^{-1} in the superconducting state may be an artifact of the Kramers-Kronig analysis. The problem in this region is that the reflectance of sample C is very close to unity. For a superconductor with a fully developed energy gap the reflectance is 1.0 for frequencies below the gap and the resulting Kramers-Kronig analysis would show a region of zero conductivity below the gap. If the reflectance is just slightly below 1.0, as is the case here, Kramers-Kronig analysis can give very large conductivities. The deviation from perfect reflectance in sample C is greater than the estimated error; however, if the sample is inhomogeneous the small deviation from 1.0 might simply be caused by a small amount of normal material in the sample. Although this has a small effect on the reflectance, the effect on the calculated conductivity can be enormous. Thus, the behavior of the conductivity below 130 cm^{-1} in the superconducting state is not certain at this point.

At higher frequencies the reflectance is much further from unity and the resulting conductivity is much more reliable. As was reported previously,¹ the background conductivity of sample A in the superconducting state exhibits a sharp upturn at around 200 cm^{-1} and actually exceeds the normal-state conductivity above 350 cm^{-1} . Although the conductivity never goes to zero at low frequencies, as one would expect in a material with a well-developed energy gap, the behavior of this polished sample might be interpreted as a hint of the onset of absorption above a gap of the order of 200 cm^{-1} .

This rapid upturn in the conductivity seen in the mechanically polished sample is not present in any of the other samples that have been studied thus far. In sample C the conductivity rises more gradually to the normal-state values, with no sign of a dramatic upturn. This slow increase is quite different from the behavior of an isotropic BCS superconductor, as discussed by Mattis and Bardeen.⁹

The sharp features in the conductivity also display interesting temperature dependences. Table I summarizes the results of fitting the peaks in the conductivity of sample C to classical oscillators:

$$\text{Re}[\sigma(\omega)] = \frac{(S\omega_{\text{TO}}^2)\omega^2\gamma}{(\omega_{\text{TO}}^2 - \omega^2)^2 + (\omega\gamma)^2}$$

Only those features which have been observed in all of the samples studied here are included. The general trend is for the peaks to soften and sharpen when the sample is cooled into the superconducting state. The apparent broadening of the feature at 279 cm^{-1} is not reliable as the fit to a classical oscillator for this feature was poor.

TABLE I. Parameters used to fit the phonon lines in the conductivity of $\text{YBa}_2\text{Cu}_3\text{O}_{7-\delta}$ (sample C) with a Lorentzian line shape.

| $T=100 \text{ K}$ | | | $T=2 \text{ K}$ | | |
|--|-------------------------------|-----|--|-------------------------------|-----|
| ω_{TO} (cm^{-1}) | γ (cm^{-1}) | S | ω_{TO} (cm^{-1}) | γ (cm^{-1}) | S |
| 155 | 3.1 | 31 | 155 | 2.4 | 31 |
| 195 | 9.6 | 3 | 194 | 2.7 | 2 |
| 279 | 18 | 6 | 277 | 21 | 10 |
| 314 | 11 | 10 | 311 | 9 | 12 |
| 532 | 57 | 2 | 534 | 50 | 3 |
| 569 | 16 | 2 | 567 | 17 | 2 |

The structures at the high-frequency end of the spectra shown here tend to have complicated, sample-dependent shapes. The feature at 569 cm^{-1} is reproducible from sample to sample, but the other features at about 530 and 610 cm^{-1} are very sample dependent.

DISCUSSION

The normal incidence reflectance of a polycrystalline anisotropic sample can be considered as a weighted average of the optical properties of a composite consisting of a portion of grains oriented with their highly conducting *ab* planes parallel to the surface and a background of less conducting material of grains with the *c* axes parallel to the surface. At low frequencies a weighted average conductivity of the components of the two individual materials is obtained. In our sample C the orientation is largely uniform with the sample surface coinciding with the *ab* plane.

At high temperature, above the superconducting transition, we find that the medium behaves like a classical plasma with a plasma frequency of 0.75 eV and a relaxation rate of 300 cm^{-1} . Together these numbers give a dc conductivity that is in good agreement with the observed dc conductivity of our sample. It is instructive to compare these numbers with estimates from other experiments.

A bulk measurement of the plasma frequency is obtained from muon spin resonance (μSR):

$$\omega_p = c/\lambda,$$

where λ is the London penetration depth. Harshman *et al.*¹⁰ find a λ of 1400 Å which yields a plasma frequency of 1.4 eV, considerably higher than the value of 0.75 eV obtained from the Drude fit above. At this point we feel that the discrepancy between these two determinations of the plasma frequency is not significant. The surface layer that the far-infrared probes may not have the density of free carriers observed in the μSR experiment. Also, Wang, Clayhold, and Ong¹¹ have shown by Hall-effect measurements that sample to sample variation in oxygen content can affect the carrier concentration without affecting the transition temperature of the material.

The plasma frequency obtained from low-frequency measurements such as far infrared or μSR is expected to be lower than what is found from an analysis of the plas-

ma edge in the near infrared. At high frequency the electrons respond with their band masses but at low frequencies the mass is renormalized by phonons and other excitations that couple to the electrons. It is found that in $\text{YBa}_2\text{Cu}_3\text{O}_7$ an edge appears at around 1 eV (Refs. 12 and 13), and is generally fit with a plasma frequency of several eV, suggesting that mass enhancements are indeed important in reducing the low-frequency plasma frequency.

It appears from the 100 K value of $1/\tau = 300 \text{ cm}^{-1}$ that the response of the free carriers at low frequency in this oriented sample is not overdamped. However, in comparison to ordinary metals this is still a large scattering rate. As pointed out by Lee and Read,¹⁴ in ordinary metals $1/\tau$ is generally less than $k_B T$ but here it is approximately $4k_B T$. It is of interest to note that this value is comparable to the characteristic energy of the gaplike feature observed in the superconducting state. The mean free path of the electrons at 100 K, assuming a Fermi velocity of $2 \times 10^7 \text{ cm sec}^{-1}$, is about 30 Å.

As the sample is cooled below the superconducting transition temperature, we observe a rapid depression of the conductivity at long wavelengths. However, this low conductivity differs from that expected for an isotropic BCS superconductor in three ways: first, we always observe some residual absorption in this gaplike region; second, except for the polished sample, the absorption does not have a sharp onset which might be associated with an energy gap; and third, the low-temperature conductivity starts to rise again below 130 cm^{-1} .

These deviations may have several causes. First, there may be some residual normal material in the outer layer of the sample probed by the far infrared. This could easily explain the residual absorption and possibly the rising conductivity below 130 cm^{-1} . The former would be the low-frequency tail of the exciton band at 0.37 eV and the latter the Drude absorption of free carriers with a relaxation time of the order of 50 cm^{-1} .

If one wishes to stay within the framework of conventional theories of superconductivity, a second possibility is extreme anisotropy of the energy gap in the *ab* plane. This could easily account for the lack of an abrupt onset of absorption in the superconducting state of the oriented samples. In a polycrystalline sample one is observing different gaps from grains oriented in different directions. Indeed, the gradual rise in the real part of the conductivity of the unpolished samples at low temperature is similar to the calculations of Maekawa, Ebisawa, and Iasua¹⁵ for highly anisotropic superconductors. Anisotropy is consistent with our observations on sample A which does seem to have an abrupt rise in the absorption at about 200 cm^{-1} . Anderson¹⁶ showed that strong disorder can wash out anisotropy in the energy gap giving rise to a single, average gap in all directions. A far-infrared measurement of a dirty, conventional, anisotropic superconductor reveals a sharp energy gap even if the sample is polycrystalline. Sample A certainly does seem to be more disordered than other samples. The much lower, flatter background conductivity in the normal state suggests a much larger scattering rate for sample A and the phonon lines are broader as well. The absence of a region of zero conductivity at low temperatures suggests that the gap is zero in

some directions; but, the μSR experiment¹⁰ seems to indicate that the anisotropy is not this large. A combination of moderate anisotropy and the presence of some normal material may be needed to reconcile these two experiments.

A third alternative is that the deviations from an isotropic BCS superconductor may be an indication that a new theory is required. Since a finite-width spectral region with zero conductivity has not yet been observed in these materials it has been argued that, at this time, there is no evidence for a gap in the high- T_c materials. Even if there is no true gap in the density of states (gapless superconductivity), any new theory must take into account the depressed conductivity in the far infrared which is observed when the sample is cooled below the superconducting transition temperature. A detailed calculation of the optical properties based on new theories of superconductivity does not exist.

For the $\text{YBa}_2\text{Cu}_3\text{O}_{7-\delta}$ structure group theory predicts 21 infrared-active phonons. The phonons are expected to fall into two natural groups, those polarized along the highly conducting *ab* plane and those polarized along the *c* axis. In La_2NiO_4 (Ref. 17) where both single-crystal and polycrystalline measurements exist it was shown that both *ab* plane and *c*-axis phonons can contribute to the features seen in reflectance of the polycrystalline samples. The reflectance spectrum of our highly oriented sample C, in the normal state, resembles the La_2NiO_4 single-crystal *ab* plane spectrum quite closely. Herr *et al.*¹³ and Wang¹⁸ have explained the very strong 250 cm^{-1} feature in $\text{La}_{2-x}\text{Sr}_x\text{O}_4$ in terms of the internal excitations of a charge transfer complex of *ab* plane atoms. This process occurs in the quasi-one-dimensional conductors where totally symmetric vibrations become electronically enhanced. If this picture is correct some of the *strongest* phonon lines could be *ab* plane excitations.

Turning to the assignments of the individual phonon frequencies we can roughly attribute the spectral features between 500 and 650 cm^{-1} to copper-oxygen stretching vibrations in analogy to other well-studied perovskites. In a structure of the complexity of the orthorhombic $\text{YBa}_2\text{Cu}_3\text{O}_7$ many nearly degenerate vibrations are expected in this region but we may tentatively assign the sharp peak at 569 cm^{-1} to a *c*-axis Cu—O stretching vibration and the weaker background from 500 to 650 cm^{-1} to the various *ab* plane stretching modes, including modes along the chains. Stavola *et al.*¹⁹ observe an infrared-active band in powder spectra of the oxygen-deficient tetragonal $\text{YBa}_2\text{Cu}_3\text{O}_6$ at 520 cm^{-1} and assign it to the *c*-axis motion of the oxygen bridging the chains. They point out that the *c* axis shortens in the orthorhombic phase and would lead to an increased frequency for this mode. Sugai²⁰ finds in a study of the phonon frequencies as a function of oxygen content in $\text{YBa}_2\text{Cu}_3\text{O}_7$ that the mode at 574 cm^{-1} moves continuously to 535 cm^{-1} as the oxygen content is reduced and the *c* axis lengthens. While our sample C is chiefly oriented with the *ab* plane parallel to the incident field a small contribution from *c*-axis polarization can be expected from the residual non-oriented fraction.

The lower-frequency modes cannot be assigned with

any confidence at this stage but they exhibit striking changes when the material becomes superconducting. There is little change in strength and slight softening on entry into the superconducting state but what is particularly outstanding is the dramatic narrowing of the two lowest peaks at low temperature, particularly the broader one at 195 cm^{-1} . The narrowing is associated with the superconducting state, and can be explained in terms of the existence of an energy gap with $2\Delta \geq 195\text{ cm}^{-1}$. Phonons with energy less than 2Δ are unable to break pairs and can propagate without scattering. In this picture we attribute most of the width of 9.6 cm^{-1} to the electron-phonon interaction. This narrowing of the two low-lying phonons is evidence for the existence of an energy gap: using this as our only criterion we can place the gap between the frequency of the phonon that narrows at 195 cm^{-1} and the lowest one that does not at 314 cm^{-1} giving a range of $2.98 \leq 2\Delta/k_B T_c \leq 4.80$.

The lowest phonon we observe, at 155 cm^{-1} , has an unusually large strength parameter, $S=31$, much too strong to be caused by simple, optically active phonons that have $S \approx 2$. It resembles the very strong line in $\text{La}_{2-x}\text{Sr}_x\text{CuO}_4$ at 250 cm^{-1} studied by Rice and Wang.¹⁸

In conclusion, measurements of the far-infrared reflectance of $\text{YBa}_2\text{Cu}_3\text{O}_{7-\delta}$ have been improved by careful sample treatment. The best results are obtained on

oriented samples that are annealed in oxygen at 900°C and cooled in oxygen and measured immediately. A true energy gap with zero conductivity below the gap frequency has not yet been observed; but, the depressed conductivity observed below 1000 cm^{-1} in the superconducting state may be due to an extremely anisotropic gap in the *ab* plane. In addition to the gaplike feature in the superconducting state, a rich spectrum of excitations is observed which are extremely strong and exhibit temperature-dependent frequencies and widths.

ACKNOWLEDGMENTS

We thank A. J. Berlinsky, C. Kallin, J. C. Carbotte, and V. J. Emery for very helpful discussions. We acknowledge valuable help with dc resistance measurements by M. Reedyk, x-ray diffraction by M. A. Crowe, and scanning electron microscope measurements by J. Carson. This research was supported at McMaster by the Natural Science and Engineering Research Council of Canada (NSERC), including infrastructure support for the Institute for Materials Research and the McMaster Nuclear Reactor, and in Florida by National Science Foundation—Solid State Chemistry—Grant No. DMR-84-16511, and by the U.S. Defence Advanced Research Projects Agency through a grant monitored by the Office of Naval Research.

- ¹D. A. Bonn, J. E. Greedan, C. V. Stager, T. Timusk, M. G. Doss, S. L. Herr, K. Kamarás, and D. B. Tanner, *Phys. Rev. Lett.* **58**, 2249 (1987).
- ²G. A. Thomas, H. K. Ng, A. J. Millis, R. N. Bhatt, R. J. Cava, E. A. Rietman, D. W. Johnson, Jr., G. P. Espinosa, and J. M. Vandenberg, *Phys. Rev. B* **36**, 846 (1987).
- ³J. M. Wrobel, S. Wang, S. Gygax, and B. P. Clayman, *Phys. Rev. B* **36**, 2368 (1987).
- ⁴L. Genzel, A. Wittlin, J. Kuhl, H. Mattausch, W. Bauhofer, and A. Simon, *Solid State Commun.* **63**, 843 (1987).
- ⁵R. T. Collins, Z. Schlesinger, R. H. Koch, r. B. Laibowitz, T. S. Plaskett, P. Freitas, W. J. Gallagher, R. L. Sandstrom, and T. R. Dinger, *Phys. Rev. Lett.* **59**, 704 (1987).
- ⁶D. A. Bonn, J. E. Greedan, C. V. Stager, T. Timusk, M. G. Doss, S. L. Herr, K. Kamarás, C. D. Porter, and D. B. Tanner, *Phys. Rev. B* **35**, 8843 (1987).
- ⁷P. E. Sulewski, T. W. Noh, J. T. McWhirter, and A. J. Sievers, *Phys. Rev. B* **36**, 5735 (1987).
- ⁸K. Kamarás, C. D. Porter, M. G. Doss, S. L. Herr, D. B. Tanner, D. A. Bonn, J. E. Greedan, A. H. O'Reilly, C. V. Stager, and T. Timusk, *Phys. Rev. Lett.* **59**, 919 (1987).
- ⁹D. C. Mattis and J. Bardeen, *Phys. Rev.* **111**, 412 (1958).
- ¹⁰D. R. Harshman, G. Aeppli, E. J. Ansaldo, B. Batlogg, J. H. Brewer, J. F. Carolan, R. J. Cava, M. Celio, A. C. D. Chaklader, W. N. Hardy, S. R. Kreitzman, G. M. Luke, D. R. Noakes, and M. Sheba *Phys. Rev. B* **36**, 2368 (1987).
- ¹¹Z. Z. Wang, J. Clayhold, and N. P. Ong (unpublished).
- ¹²Joseph Orenstein, G. A. Thomas, D. H. Rapkine, C. G. Bethea, B. F. Levine, R. J. Cava, E. A. Reitman, and D. W. Johnson, Jr., *Phys. Rev. B* **36**, 729 (1987).
- ¹³S. L. Herr, K. Kamarás, C. D. Porter, M. G. Doss, D. B. Tanner, D. A. Bonn, J. E. Greedan, C. V. Stager, and T. Timusk, *Phys. Rev. B* **36**, 733 (1987).
- ¹⁴P. A. Lee and N. Read, *Phys. Rev. Lett.* **58**, 2691 (1987).
- ¹⁵S. Maekawa, H. Ebisawa, and Y. Isawa, *Jpn. J. Appl. Phys. Lett.* **26**, L468 (1987); **26**, L992 (1987).
- ¹⁶P. W. Anderson, *J. Phys. Chem. Solids* **11**, 26 (1959).
- ¹⁷J. Bassat, P. Odier, and F. Gervais, *Phys. Rev. B* **35**, 7126 (1987).
- ¹⁸M. J. Rice and Y. R. Wang (unpublished).
- ¹⁹M. Stavola, D. M. Krol, W. Weber, S. A. Sunshine, A. Jayaraman, G. A. Kouroukis, R. J. Cava, and E. A. Reitman, *Phys. Rev. B* **36**, 850 (1987).
- ²⁰S. Sugai (unpublished).